

## Computer Simulation of Sensing Current Effects on the Magnetic and Magnetoresistance Properties of a Crossed Spin-Valve Head

S. H. Lim, S. H. Han, K. H. Shin and H. J. Kim

*Thin Film Technology Research Center, Korea Institute of Science and Technology, P.O. Box 131, Cheongryang, Seoul 130-650, Korea*

(Received 26 April 2000)

Computer simulation of sensing current effects on the magnetic and magnetoresistance properties of a crossed spin-valve head is carried out. The spin-valve head has the following layer structure: Ta (8.0 nm)/NiMn (25 nm)/NiFe (2.5 nm)/Cu (3.0 nm)/NiFe (5.5 nm)/Ta (3.0 nm), and it is 1500 nm long and 600 nm wide. Even with a high pinning field of 300 Oe and a high hard-biased field of 50 Oe, the ideal crossed spin-valve structure, which is essential to the symmetry of the output signal and hence high density recording, is not realized mainly due to large interlayer magnetostatic interactions. This problem is solved by applying a suitable magnitude of sensing currents along the length direction generating magnetic fields in the width direction. The ideal spin-valve head is expected to show good symmetry of the output signal. This has not been shown explicitly in the present simulation, however. The reason for this is possibly related to the simple assumption used in this calculation that each magnetic layer consists of a single domain.

### 1. Introduction

High sensitivity and good linear response are very important factors as a read head for the realization of high density recording. Between these two, the linearity of output signals is probably more important than the sensitivity considering recent advances in the field of spin-valve multilayers with high magnetoresistance [1, 2]. Linear response of a spin-valve head is closely related to its magnetic configuration, specifically, the magnetization directions of the pinned and free layers. It is well-known that, although the sensitivity of a spin-valve head is highest when the directions of the two magnetizations and applied field ( $H_a$ ) are all co-linear, the best linearity is achieved in a so-called crossed spin-valve where the magnetic spin in the pinned layer is directed toward the width direction and that in the free layer toward the length direction. This is the magnetic configuration that is being used in magnetic recording. The direction of  $H_a$  (more specifically, the stray field from a recorded bit pattern) in magnetic recording is perpendicular to that of free layer magnetization.

The crossed spin configuration is not "natural" since the spin direction in the pinned layer must overcome the self-demagnetization torque. The realization of this spin structure is assisted by the exchange-biased field (often called the pinning field,  $H_p$ ) acting on the pinned layer from an adjacent antiferromagnetic pinning layer. Even with this assistance, however, it is not easy to achieve the ideal crossed spin configuration, causing the asymmetry of out-

put signal [3, 4]. This problem becomes more prominent when the size of the sensor element is smaller, since the contribution to the total energy by the magnetostatic interactions increases with the decrease of the sensor size [5, 6].

There are many other parameters, apart from the sensor size, in determining the magnetic configuration. These parameters may include the exchange-biased field, the hard-biased field ( $H_{h-b}$ ) used to form a single domain structure in the free layer, the uniaxial anisotropy, the exchange field between the two magnetic layers, and the sensing current ( $i_s$ ). Systematic work is necessary to sort out the role of the parameters, and, as a first attempt, effects of  $H_{h-b}$  were previously investigated by the present authors on the magnetic and magnetoresistance properties of a crossed spin-valve head [7]. Within the model and parameters used previously, the ideal crossed spin-valve structure was not realized, although the ideality was improved by the existence of  $H_{h-b}$ . The sensing current, which is known to assist the formation of the crossed spin-valve structure, was not taken into account in the previous work. The aim of the present work is to investigate the effects of the sensing current on the magnetic properties, including magnetoresistance, of a spin-valve head. Work on the sensing current effects in spin-valves was done previously. However, no detailed investigation on the effects of the sensing currents of the magnetic properties of the constituent layers was done, to the best of our knowledge. Effects of high current density on the electromigration, self-fields and thermal heating were examined by Kos *et al.* [8] for a set of spin-valve heads for magnetic

recording. The magnetic configuration of the spin-valve examined by Russek *et al.* [9] was relevant to an MRAM device where the pinning field and the applied field are all parallel to the length direction. Various spin configurations were considered by Portier *et al.* [10] except for the current spin-valve structure, and the sample size considered was rather large being  $10 \mu\text{m} \times 10 \mu\text{m}$ .

## 2. Model and Computation

The model used here was the same as that used previously, so for details, refer to reference [7]. Briefly, each magnetic layer consists of a single domain, indicating that the magnetization is uniform within a layer. Magnetic layers are coupled through the magnetostatic and interlayer exchange interactions. The spin-valve modeled in this work is Ta/NiMn/NiFe/Cu/NiFe/Ta. The modeled spin-valve structure is shown in Fig. 1, together with the definition of the axes. The sensor is 600 nm wide and 1500 nm long. The other parameters including the dimensions, and magnetic and electrical properties are summarized in Table 1. The resistivity values given in the table for the Ta, NiFe and Cu films were taken from the work of Yamada *et al.* [11] who determined the resistivity values by analyzing the variation of the sheet conductance with film thickness based on the Fuchs-Namba model [12].

With no data available in the literature for the NiMn layer, at least to our knowledge, the resistivity of the NiMn

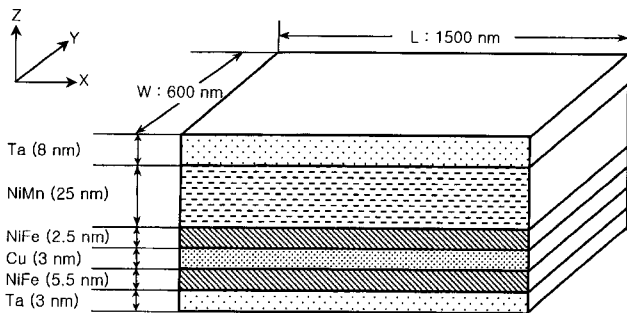


Fig. 1. The spin-valve structure modeled in this work, together with the definition of the axes.

Table 1. The thickness, saturation magnetization and the resistivity of the constituent layers of the spin-valve modeled in this work

Layer Type	Thickness (nm)	Saturation Magnetization (emu/cc)	Resistivity ( $\mu\Omega\text{cm}$ )
Ta (I)	8.0	0	180
NiMn	25.0	0	180
NiFe (pinned)	2.5	800	40
Cu	3.0	0	6.5 or 13.0
NiFe (free)	5.5	800	40
Ta (II)	3.0	0	180

layer was assumed to be equal to that of the Ta layer. This assumption is considered to be reasonable, since, in a multi-layer spin-valve containing both Ta and NiMn layers, the current densities of the two layers are identical to each other [13]. The antiferromagnetic layer is assumed to be pinned very strongly in the width direction, so its magnetization is essentially fixed. The unidirectional exchange-biased field is 150 or 300 Oe and points in the +y direction. In the pinned and free layers, the uniaxial induced anisotropy with a strength of 5 Oe is assumed to be formed in the x direction. Unidirectional  $H_{h-b}$  is applied to both the pinned and free layers in the +x direction and its magnitude is 25 or 50 Oe. The value of  $i_s$  ranges from 0 to 6 mA, and its direction is in the +x direction. The change of the magnetoresistance is calculated by using the expression  $\Delta R = 1 - \cos\theta$ , where  $\theta$  is the angle between the magnetization directions of the two magnetic layers. The magnetic field is applied in the width direction (y axis) and is cycled between +500 and -500 Oe, in order to observe how the magnetic and magnetoresistive properties vary with  $H_a$ .

## 3. Results and Discussion

In Fig. 2 are shown the results for the magnetization directions of the pinned and free layers as a function of  $i_s$  before applying magnetic field (at  $H_a=0$ ) to see the initial magnetization configuration of the spin-valve. The value of  $H_{h-b}$  is fixed at 25 Oe, but two different values of  $H_p$  (150 and 300 Oe) are considered to examine its dependence of the initial magnetization configuration. With the present magnetic parameters used here, the magnetization is always confined to the xy plane. This is readily expected from a very large demagnetization factor in the thickness (z) direction. So, the magnetization direction can be specified by an angle in the xy plane and the angle used in this work is defined to be between the magnetization direction and the +x axis. The symbols,  $\theta_p$  and  $\theta_f$ , are used to denote the magnetization angles of the pinned and free layers, respectively.

In the case of  $H_p=150$  Oe, the magnetization directions of the pinned and free layers are respectively away from the pinning (+y) and the easy (x) directions at  $i_s=0$ , the angles being  $98^\circ$  (the pinned layer) and  $-22^\circ$  (the free layer). The canting of the pinned layer, in spite of a rather strong pinning field (150 Oe), is mainly due to the magnetostatic field, particularly the self-demagnetization field which acts to rotate the spin in the length direction. The self-demagnetization field is dependent on the layer geometry, and is related to the shape anisotropy, the magnitude of which is equal to the difference of the self-demagnetization fields in the x and y directions (note that the spins reside in the xy plane only in this work). The values of the shape anisotropy are 27 and 55 Oe, respectively, for the pinned and free layers. In the case of the free layer, the demagnetization field,

together with the uniaxial anisotropy field, tries to align the spin in the length direction. However, the interlayer magnetostatic field (due to the stray field) causes the magnetization away from the easy axis. The free layer deviates more from the ideality than the pinned one, and this can be expected from the strong pinning field acting on the latter layer. Since the magnetization directions of the two magnetic layers deviate substantially from the ideal crossed spin-valve structure, the output signal is expected to be quite asymmetrical in this case.

As the value of  $i_s$  increases, the free layer spin rotates towards the  $+x$  direction, but the pinned layer one is further away from the  $+y$  direction. This change of  $\theta_p$  and  $\theta_f$  can be explained from the direction of the magnetic field generated by  $i_s$  ( $H_i$ ). With the present spin-valve structure and the direction of  $i_s$  ( $+x$ ), the directions of  $H_i$  point to the  $-y$  and  $+y$  directions in the pinned and free layers, respectively. The magnitude of  $H_i$  is linearly proportional to  $i_s$  and is rather large, being 118.4 Oe/mA for the pinned layer and 85.6 Oe/mA for the free layer. At low  $i_s$  values below 0.5 mA, the variation of  $\theta_f$  with  $i_s$  is greater than that of  $\theta_p$  due to the strong  $H_p$  acting on the pinned layer, although a higher value of  $H_i$  is generated in the pinned layer than in the free layer. This difference in the  $i_s$  dependence of  $\theta_p$  and  $\theta_f$  in the low  $i_s$  range results in the improvement of the ideal spin structure. In other words, the deviation from the ideality decreases with the increase of  $i_s$ . The ideal crossed spin-valve configuration, however, cannot be realized. The changes of  $\theta_p$  and  $\theta_f$  with  $i_s$  are relatively small at low  $i_s$  values below 0.6 mA. In the range of 0.6 to 1.0 mA, however, the magnetization direction varies with  $i_s$  significantly, since  $H_i$  prevails in this range. Resultantly, the spins in the two magnetic layers are aligned in the  $H_i$  directions; namely, the pinned layer spin in the  $-y$  direction and the free layer in the  $+y$  direction. The large change of the magnetization direction of the free layer in this  $i_s$  range can easily be understood, since the value of  $H_i$  in this layer is substantially larger ( $\sim 86$  Oe at 1 mA, for example) than the other fields. On the other hand, the spin rotation towards the  $-y$  direction in the pinned layer appears hard to understand considering that the value of  $H_p$  (150 Oe) is larger than that of  $H_i$  ( $\sim 120$  Oe at 1 mA). The spin rotation of the pinned layer, however, is assisted by a large inter-layer magnetostatic field from the free layer which acts to rotate the pinned layer spin to the  $-y$  direction.

In the case of  $H_p=300$  Oe, the change of the magnetization direction with  $i_s$  is qualitatively similar to that for  $H_p=150$  Oe. One main difference is that, at  $i_s$  values below 1.0 mA, the free layer spin rotates slowly to the  $+x$  direction, and the pinned layer spin remains nearly constant, pointing in the  $+y$  direction, due to the strong pinning field. This variation of the spin direction with  $i_s$  results in the realization of nearly ideal crossed spin-valve structure. The most ideal spin configuration is obtained at  $i_s=0.6$  mA where  $\theta_p=98^\circ$  and  $\theta_f=0^\circ$ . With the further increase of  $i_s$ ,

large changes in  $\theta_p$  and  $\theta_f$  are observed. Again, a steep change of  $\theta_p$  occurs at a  $H_i$  value (180~240 Oe in the  $i_s$  range 1.5~2 mA) substantially smaller than  $H_p$  (300 Oe). This is due to a large interlayer magnetostatic field acting on the pinned layer from the free layer which tries to rotate the pinned layer spin to the  $-y$  direction. It is worth noting a very steep change of  $\theta_p$  (similar to the  $\lambda$ -like change) at  $i_s \cong 2.0$  mA. The peak occurs at  $i_s=1.897$  mA where  $\theta_p=326^\circ$  ( $-34^\circ$ ) and  $\theta_f=85^\circ$ , both spins pointing to the  $+x$  direction. At an  $i_s$  value just below the peak, say  $i_s=1.896$  mA,  $\theta_p=227^\circ$  ( $-133^\circ$ ) and  $\theta_f=67^\circ$ . These sudden changes of  $\theta_p$  and  $\theta_f$  (particularly  $\theta_p$ ) can be explained as follows. In the presence of  $H_{b-h}$ , the free layer spin resides in the  $+x$  hemisphere and this causes the pinned layer spin to stay in the  $-x$  hemisphere, since the interlayer magnetostatic field is larger than  $H_{b-h}$ . However, as  $\theta_f$  approaches  $90^\circ$ , the field component in the  $-x$  direction by the interlayer magnetostatic interaction acting on the pinned layer from the free layer becomes small, eventually this field component becoming smaller than  $H_{b-h}$  causing the pinned layer spin to jump from the  $-x$  to  $+x$  hemisphere.

Although the  $i_s$  range investigated in this work is quite wide up to 6 mA, the spin configuration close to the crossed spin valve structure is limited to a small  $i_s$  region. This is quite different from the actual situation where the value of  $i_s$  is known to be several mA, indicating that the parameters used here are not very realistic. In an effort to rectify this situation, the value of  $H_{b-h}$  is increased from 25 to 50 Oe, and the resistivity of the Cu layer ( $\rho_{Cu}$ ) is doubled

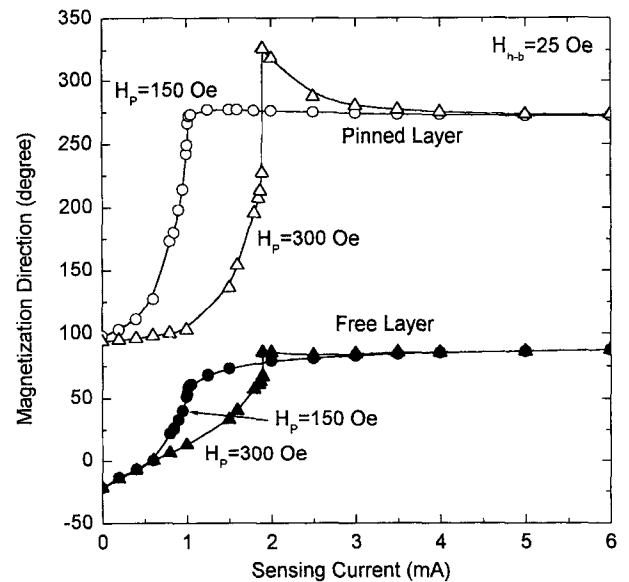


Fig. 2. Initial magnetization directions of the pinned and free layers measured at zero applied field as a function of the sensing current. The value of  $H_{b-h}$  is fixed at 25 Oe, but two different values of  $H_p$  (150 and 300 Oe) are considered to examine its dependence of the initial magnetization configuration. The spins reside in the  $xy$  plane and the angle is between the magnetization direction and the  $+x$  axis.

from 6.5 to 13.0  $\mu\Omega\text{cm}$ . This increase of the resistivity has an effect of decreasing the  $H_i$  by half; specifically, the increment of  $H_i$  is 59.2 Oe/mA for the pinned layer and 42.8 Oe/mA for the free layer. In Fig. 3 are shown the results for the magnetization directions of the pinned and free layers as a function of  $i_s$  before applying magnetic field (at  $H_a=0$ ). In order to see the resistivity effect more clearly, the results at the low resistivity are also shown in the figure. The pinned layer spin points to the +y direction due to the strong pinning field. The free layer spin, however, is deviated from the +x direction in spite of the high  $H_{b-h}$  value. This is of course due to the interlayer magnetostatic field acting on the free layer in the -y direction. The pinned layer spin remains nearly unchanged up to  $i_s=1$  mA again due to the strong pinning field, but the free layer spin rotates towards the +x direction with the increase of  $i_s$ . As a result of this, the ideal crossed spin-valve structure is achieved; at  $i_s=0.6\sim 0.8$  mA when  $\rho_{\text{Cu}}=6.5 \mu\Omega\text{cm}$ , and at  $i_s=0.8\sim 1.0$  mA when  $\rho_{\text{Cu}}=13.0 \mu\Omega\text{cm}$ . It is worth noting here that spins in both the pinned and free layers stay in the +x hemisphere due to the high  $H_{b-h}$  value. This is to be compared with the previous case for  $H_{b-h}=25$  Oe where the pinned layer spin usually stays in the -x hemisphere.

Magnetic field is cycled between +500 and -500 Oe in the width direction in order to see the dependence of the magnetic and magnetoresistive properties on  $H_a$ . In Fig. 4 are shown the results for the magnetization directions of both the pinned and free layers as a function of  $H_a$  during the whole cycle at fixed  $i_s$  values of 0, 0.6, 1.25 and 2.0 mA. The other parameters used are;  $H_{b-h}=50$  Oe,  $H_p=300$

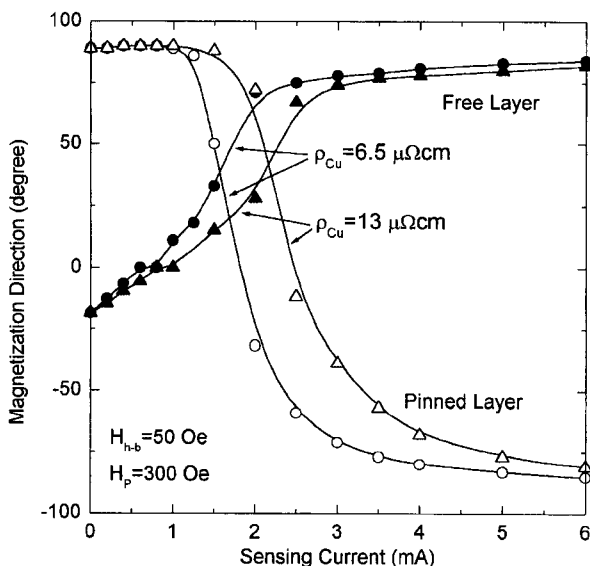


Fig. 3. Initial magnetization directions of the pinned and free layers measured at zero applied field as a function of the sensing current. The values of  $H_{b-h}$  and  $H_p$  are fixed at 50 and 300 Oe, respectively, but two different values of Cu resistivity are considered to examine its dependence of the initial magnetization configuration. The spins reside in the xy plane and the angle is between the magnetization direction and the +x axis.

Oe, and  $\rho_{\text{Cu}}=6.5 \mu\Omega\text{cm}$ . In the case of  $i_s=0$ , the magnetizations of both the pinned and free layers point to the directions close to +y at high  $H_a$  values, indicating that the Zeeman energy prevails in this region. Even at the highest applied field of 500 Oe, however, both spins do not point to the  $H_a$  (+y) direction exactly, the deviation from the +y direction being greater in the free layer than in the pinned layer. As  $H_a$  decreases, the magnetization direction rotates further away from the +y direction, principally due to the shape anisotropy. The rotation of the free layer is larger than that of the pinned layer, and this can be understood from the existence of the pinning field in the pinned layer. This rotation of the free layer, in turn, causes to rotate the pinned layer into an angle even close to  $90^\circ$ , through interlayer magnetostatic interactions. As  $\theta_f$  reaches  $0^\circ$ , a plateau occurs where  $\theta_f$  does not vary with  $H_a$ . This plateau, which occurs in the  $H_a$  range  $44 \text{ Oe} \leq H_a \leq 68 \text{ Oe}$ , can be explained by the stabilization of the free layer by the self-demagnetization field, the uniaxial field and the hard-biased field. A similar plateau is also observed when  $\theta_p=0^\circ$  (in this case  $\theta_f \cong -90^\circ$ ) in the  $H_a$  range  $-428 \text{ Oe} \leq H_a \leq -416 \text{ Oe}$ . The reason for the formation of this plateau is the same for the  $\theta_f=0^\circ$  case. The  $H_a$  dependence of  $\theta_p$  and  $\theta_f$  in the presence of  $i_s$  is similar to that in the case of  $i_s=0$ . One most obvious feature is that, as  $i_s$  increases, the spin in the pinned layer begins to rotate to the -y direction at a small Zeeman force component in this direction, but the spin in the free layer rotates at a high Zeeman force. At  $i_s=2.0$ , for example, the pinned layer spin deviates significantly from the +y direction even at positive  $H_a$  values, causing the pinned layer to switch earlier than the free layer. This  $H_a$  dependence of  $\theta_p$  and  $\theta_f$  as a function of  $i_s$  can be expected from the direction of  $H_i$  in each layer (the -y direction in the pinned layer and the +y direction in the free layer). It is of interest to observe a broad maximum in the  $\theta_p$ - $H_a$  curve at  $i_s=1.25$ , and a similar minimum in the  $\theta_p$ - $H_a$  curve at  $i_s=2.0$ . This appears strange being against the Zeeman energy. As the Zeeman force component in the -y direction increases, the spin direction rotates back to the +y direction in the case of the broad maximum in the  $\theta_p$ - $H_a$  curve at  $i_s=1.25$ , and the spin direction is away from the -y direction in the case of the minimum in the  $\theta_p$ - $H_a$  curve at  $i_s=2.0$ . This strange behavior is due to a strong interlayer magnetostatic field. For example, the maximum in the  $\theta_p$ - $H_a$  curve can be explained by a strong interlayer magnetostatic field acting on the pinned layer in the -x direction from the free layer which points to the +x direction.

The  $H_a$  dependence of magnetization and magnetoresistance can be evaluated from the results shown in Fig. 4 for  $\theta_p$  and  $\theta_f$  as a function of  $H_a$ , and the results for these properties are shown in Fig. 5 (magnetization) and Fig. 6 (magnetoresistance). The results are shown at fixed  $i_s$  values of 0, 0.6, 1.25 and 2.0 mA, and the parameters used are the same with those in Fig. 4. A progressive change occurs for the magnetization curves for  $i_s=0, 0.6$  and 1.25. As  $H_a$

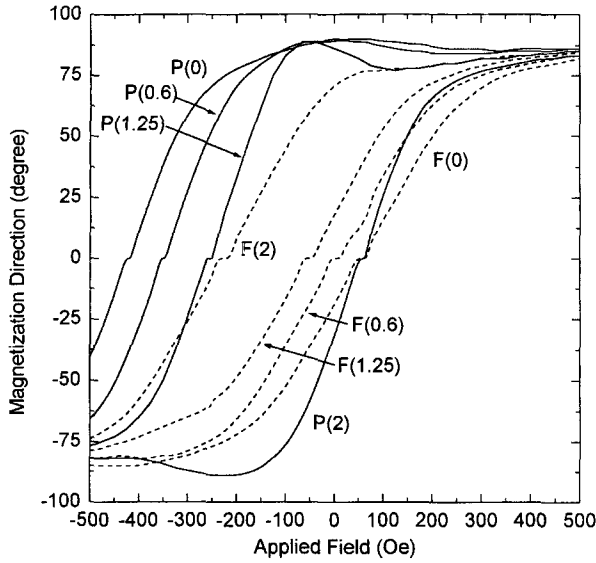


Fig. 4. Magnetization directions of the pinned and free layers during the whole cycle of applied field at various sensing currents of 0, 0.6, 1.25 and 2.0 mA. The spins reside in the  $xy$  plane and the angle is between the magnetization direction and the  $+x$  axis. The letters P and F, respectively, denote the pinned and free layers.

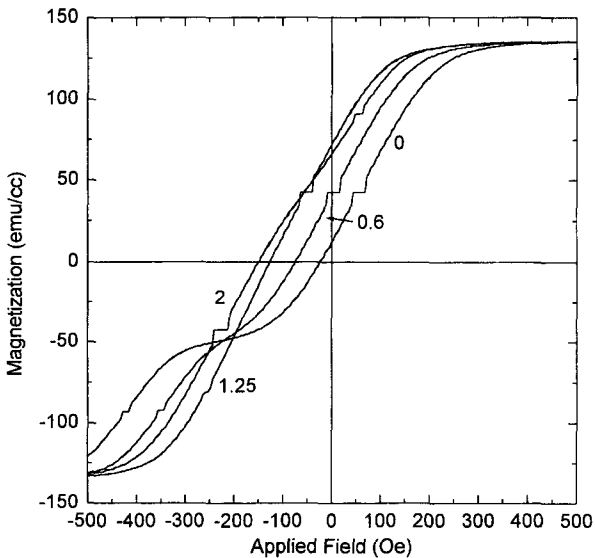


Fig. 5. M-H hysteresis loops at various sensing currents of 0, 0.6, 1.25 and 2.0 mA. The numbers at the curves denote the values of the sensing current.

decreases from the maximum applied field of 500 Oe, the value of  $H_a$  at which magnetization begins to decrease is larger at smaller  $i_s$  values. This is because the magnetization change in this region is dominated by the free layer, and the magnetization rotation of the free layer is hindered by  $H_i$ , whose direction points to the  $+y$  direction. The saturation in the negative direction, however, is reached more easily at larger  $i_s$  values, since, in this  $H_a$  range, the magnetization change is dominated by the pinned layer, and the magnetization rotation of the pinned layer is assisted by  $H_i$ , whose

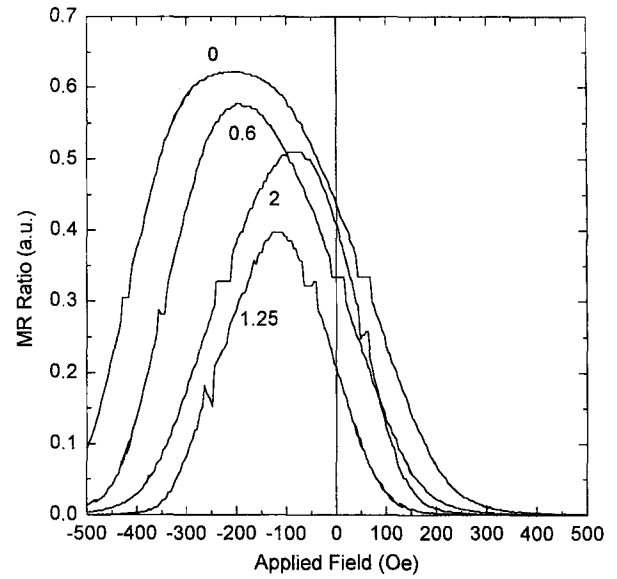


Fig. 6. The giant magnetoresistance curves at various sensing currents of 0, 0.6, 1.25 and 2.0 mA. The numbers at the curves denote the values of the sensing current.

direction points to the  $-y$  direction. On the other hand, the magnetization curve at  $i_s=2.0$  is different from the other curves for the lower  $i_s$  values, mainly because the pinned layer begins to switch earlier than the free layer. In all the cases, no hysteresis is observed, indicating that the magnetization occurs mainly by a continuous rotation of magnetization, not by a sudden spin flip. This can be expected in a crossed spin-valve structure.

Let us finally consider the magnetoresistance behavior. The magnetoresistance near  $H_a \cong 0$  which is practically important is dominated by the rotation of the free layer at  $i_s = 0, 0.6$  and  $1.25$ . In the case of  $i_s=2.0$ , however, it is dominated by the pinned layer. Considering this spin behavior, it is rather unexpected that the magnetoresistance is also large at this sensing current. This situation is not realistic and will not be considered in the following discussion. For the given  $H_a$  cycle, the magnetoresistance ratio is highest at  $i_s=0$ , and it decreases with increasing  $i_s$ . The best linearity is expected to be observed at  $i_s=0.6$  where the ideal spin-valve structure is achieved. However, it is hard to conclude from the present results, since the plateau exists at  $H_a \cong 0$ . The existence of the plateau, which is not usually observed in a real crossed spin-valve, may be due to the assumption of the present model that each layer consists of a single domain. Although the single domain assumption is simple and efficient from the calculation point of view, and has been used successfully in many micromagnetic simulations, the present result may indicate that a caution should be exerted to use this simple assumption. If the plateau is not considered and this region is interpolated by considering the results outside the plateau, it seems that the best linearity is obtained at  $i_s=0.6$  where the ideal spin-valve structure is achieved at  $H_a=0$

#### 4. Conclusions

Computer simulation has been carried out in this work to examine the effects of sensing current on the magnetic and magnetoresistance properties of a crossed spin-valve head. Particular emphasis has been placed on the symmetry of the output signal, which is essential to high density recording. The spin-valve head modeled in the calculation is Ta (8.0 nm)/NiMn (25 nm)/NiFe (2.5 nm)/Cu (3.0nm)/NiFe (5.5 nm)/Ta (3.0 nm), with a length of 1500 nm and a width of 600 nm. A simple model has been used in this work, where each magnetic layer consists of a single domain, and the magnetoresistance is calculated by using the expression  $\Delta R = 1 - \cos\theta$ , where  $\theta$  is the angle between the magnetization directions of the two magnetic layers. The patterned head with small dimensions possesses large magnetostatic interactions so that the ideal crossed spin-valve structure is not realized even with a high pinning field of 300 Oe and a high hard-biased field of 50 Oe. This problem is solved with the application of sensing currents along the length direction generating magnetic fields in the width direction. The best signal symmetry is expected at the condition showing the ideal spin-valve structure. However, this has not been demonstrated in the present simulation, since a plateau exists in the practically important region of  $H_a \cong 0$ . The reason for the existence of the plateau is possibly related to the simple assumption used in this model that each magnetic layer consists of a single domain. The present result may indicate that a caution should be exerted to use the simple assumption of the single domain model.

#### Acknowledgment

The simulation was performed with a program developed

at NIST by Dr. John Oti.

#### References

- [1] H. Iwasaki, H. Fukuzawa, Y. Kamiguchi, H. N. Fuke, K. Saito, K. Koi and M. Sahashi, International Magnetism Conference, May 18-21, 1999, Kyongju, Korea, Paper No. BA-04.
- [2] Y. Kamiguchi, H. Yuasa, H. Fukuzawa, K. Kouji, H. Iwasaki and M. Sahashi, International Magnetism Conference, May 18-21, 1999, Kyongju, Korea, Paper No. DB-01.
- [3] K. Yamada, H. Kanai, Y. Uehara and J. Toda, IEEE Trans. Magn., **34**, 1447 (1998).
- [4] H. Kanai, K. Yamada, M. Kanamine and J. Toda, IEEE Trans. Magn., **34**, 1498 (1998).
- [5] R. W. Cross, Y. Kim, J. O. Oti and S. E. Russek, Appl. Phys. Lett., **69**, 3935 (1996).
- [6] J. O. Oti, R. W. Cross, S. E. Russek and Y. K. Kim, J. Appl. Phys., **79**, 6386 (1996).
- [7] S. H. Lim, K. H. Shin, K. Y. Kim, S. H. Han and H. J. Kim, J. Magnetism, **5**, 19 (2000).
- [8] A. B. Kos, S. E. Russek, Y. K. Kim and R. W. Cross, IEEE Trans. Magn., **33**, 3541 (1997).
- [9] S. E. Russek, J. O. Oti, Y. K. Kim and R. W. Cross, IEEE Trans. Magn., **33**, 3292 (1997).
- [10] X. Portier, A. K. Petford-Long, T. C. Anthony and J. A. Brug, J. Magn. Magn. Mater., **187**, 145 (1998).
- [11] K. Yamada, W. E. Bailey, C. Fery and S. X. Wang, IEEE Trans. Magn., **35**, 2979 (1999).
- [12] Y. Namba, Jpn. J. Appl. Phys., **9**, 1326 (1970).
- [13] I.-F. Tsu, C. Chang and H. S. Edelman, MRS99 Spring Meeting, April 6-8, 1999, San Francisco, USA.